Formation, Characterization, and Functions of Ceramic Nanotubes

Motonari Adachi, Yusuke Murata, Issei Okada, and Susumu Yoshikawa

Institute of Advanced Energy, Kyoto University, Uji, Kyoto 611-0011, Japan
Fax: 81-774-38-3508, e-mail: adachi@iae.kyoto-u.ac.jp

Formation method for ceramic nanotiubes of many kinds of quadrivalent metal oxides was found using surfactant-assisted templating mechanism in laurylamine / metal alkoxides system. Titania nanotubes have mono-crystalline anatase structure and showed the highest photo-catalytic activity among the commercially available nano-size photo-catalytic titania materials. The dye-sensitized solar cell system using the highly photo-catalytic titania nanotubes showed more than two times higher short-circuit current density than the cell made of P-25 in the thin film thickness region. The nanotubes made of ceria were successfully synthesized and showed high surface area in comparison with the commercially available ceria particles.
Key words: ceramic nanotube, formation method, templating mechanism, photo-catalytic activity, dye-sensitized solar cell

1. INTRODUCTION

Novel performance through nano-structuring has been recognized in many branches of science in the latter half of twenty century.

In order to realize the tremendous potential of nanostructure science and technology, extremely important challenges are to exploit synthetic methods for structures regulated in atomic scale and to construct materials across the hierarchy of length scale from atomic to mesoscopic, and/or to macroscopic scale.

Artificial synthetic methods of nano-scale materials and hierarchical assembles of them have been investigated using self-organized mechanism by chemical and bio-inspired methods. In 1992, researchers at Mobil demonstrated mesoporous silicate and alminosilicate materials (M41S)[1,2] by a surfactant-assisted templating mechanism using molecular assemblies as a template. MCM41, one member of the M41S family, has a regular hexagonal array of uniform pore size (15 to 100 Å). Thereafter, a variety of mesoporous materials have been synthesized using molecular assemblies. These materials have been obtained as integrated forms of unit structure. Single or bundles of a few silica-nanotubes, however, have not yet been synthesized by a surfactant assisted templating mechanism until we succeeded in formation of silica nanotubes. [3,4] .

Single hollow nanotubes have attracted a great deal of attention in both fundamental and industrial studies [5-7]. They have potential applications in the fields such as electronics, optics, advanced catalysis and energy storage/conversion. They have novel properties, and could be used to make functional materials using both their inner and outer spaces. Nakamura and Matsui [8] obtained silica gel tubes by the sol-gel method. Lin and Mou [9] and Trau et al. [10] synthesized a tubular structure composed of MCM41. Masuda et al. [11,12] synthesized a highly ordered nanochannel-array in anodic alminium oxide, and various ceramics tubes were formed using anodic almina nanochannel-array as a template. Mann et al. [13] and Shinkai et al. [14] made silica nanotubes using tobacco mosaic virus and organic nanotubes as a template, respectively.

However, their diameters were all sub-micron to micron size, much larger than nano-size, and the structure is polycrystal. From the view points of understanding the formation mechanism and also making new materials, it was interesting to examine whether single silica nanotubes of real nano-size or bundles of a few of them can be formed through a surfactant-assisted templating mechanism.

There is still no sufficient general model for a mechanistic understanding of the synthesis processes, which is the key to the rational design of new materials. The main reason preventing the elucidation of the formation processes is as follows: In most of the formations of mesoporous materials by the templating mechanism, either precipitation occurs in the early stage of the formation processes or the materials are synthesized under conditions of high surfactant concentration. These circumstances make it difficult to measure the variation in shape and size of produced silica materials during the microstructure formation.

Our strategy was to find an appropriate formation system in which gelation occurs homogeneously in dilute conditions without precipitation of silicates. The shape and size of the produced silica materials can be measured by small angle X-ray scattering (SAXS) during the formation process, especially in the early stage of microstructure formation. We discovered a laurylamine hydrochloricde (LAHC)/tetraethoxysilane (TEOS) system, in which gelation occurs homogeneously, and succeeded in forming single silica nanotubes instead of integrated ordered silica materials. We extended the method to synthesize titania nanotubes using LAHC / tetraisopropylorthotitanate (TIPT) with acetylacetone (ACA) system last year [15].

In this paper, we present the preparation of titania nanotubes and a mono-crystal structure of these nanotubes characterized by transmission electron microscopy (TEM) images, together with electron diffraction, X-ray diffraction and nitrogen adsorption isotherms. We applied this highly photo-catalytic titania nanotubes for a semiconductor thin film electrode in dye-sensitized solar cells and attained more than two times higher efficiency of the thin film electrode made of

titania nanotubes, comparing with those of P-25 in the thin film region. Further, the nanotubes made of ceria were successfully synthesized and showed high surface area in comparison with the commercially available ceria particles.

2. EXPERIMENTAL

Formation of Titania Nanotubes

We used mainly the LAHC / TIPT with ACA system in preparation of titania nanotubes by sol-gel method. In some cases, octadecylamine (ODA) was used as a surfactant. The reaction behavior in the ODA system was almost the same as that in the LAHC system. When TIPT was mixed with the same moles of ACA, ACA coordinate to titanium atom, letting one isopropoxyl group unbound. The coordination number of titanium atom changed from 4 to 5, resulting in a color change from colorless to yellow. The experimental procedure was described in the previous paper [15]. Characterization of the produced materials was made by small angle X-ray scattering (SAXS), X-ray diffraction (XRD), transmission electron microscopy (TEM), electron diffraction, scanning electron microscopy (SEM), and isotherm of nitrogen adsorption. The photo-catalytic activity of titania nanotubes was measured through the formation rate of I_3^- due to the oxidation of I^- to I_2. The produced titania compounds were ground in a mortar made of agate, and 50 mg of them were suspended in 10 ml of 0.2 M KI aqueous solution by magnetic stirring. The reaction was carried out under the irradiation of UV-light of 365 nm.

Preparation of Titania Thin Films and Solar Cells

Thin titania films were made by applying a titania sample on a fluorine doped conducting tin oxide glass plate. After drying, the sample was calcined at 723 K for 30 minutes. Dye was introduced to the titania thin films by adsorption. Cis-di(thiocyanate)bis(2,2'-bipyridyl-4,4'-di-carboxylate) ruthenium(II) (R535) produced by Grätzel's group [16] was used as the dye. The solar cell comprised titania thin film electrode on a conducting glass plate, a platinum electrode and electrolyte between the titania thin film and the platinum. We used 0.03 M iodine in 0.3 M lithium iodide in 3-methyl-2-oxazolidinone (NMO)/acetonitrile solution as the electrolyte. The volume ratio of NMO to acetonitrile was 1/9. The photo-current-voltage characteristics were measured using a potentiostat (Hokuto Denko HA-501G, HB-105) by irradiating with simulated solar light, i.e., AM1.5 100mW/cm² (ORIEL 1000W 91192). The cell size was 1cm² or 0.25 cm². Cells made of P-25 were also prepared after Grätzel's method [16] for comparison, and the photo-current-voltage characteristics were measured under the same conditions.

Formation of Cerium Nanotubes

Cerium nanotubes were synthesized as follows. Tetra-buthoxycerium in isopropanol/methoxypropanol mixed solution was used. (0.5mol/kg) ACA was added to the solution. The mol ratio of metal to ACA was unity. Then, the solution was mixed with 0.1 M LAHC aqueous solution at 313 K. The mol ratio of metal to LAHC was 8. After the solution was kept at 313 K for 3 day, the reaction was carried out at 353 K for 10 days. The sample was dried at 353 K and was calcined at 773 K for 4 hours.

3. RESULTS AND DISCUSSION

Titania Nanotubes

The reaction in the mixed solution of LAHC aqueous solution and TIPT modified with ACA proceeded as follows. When the

two solutions were mixed, precipitates were formed. The solution was stirred further to dissolve the precipitates completely
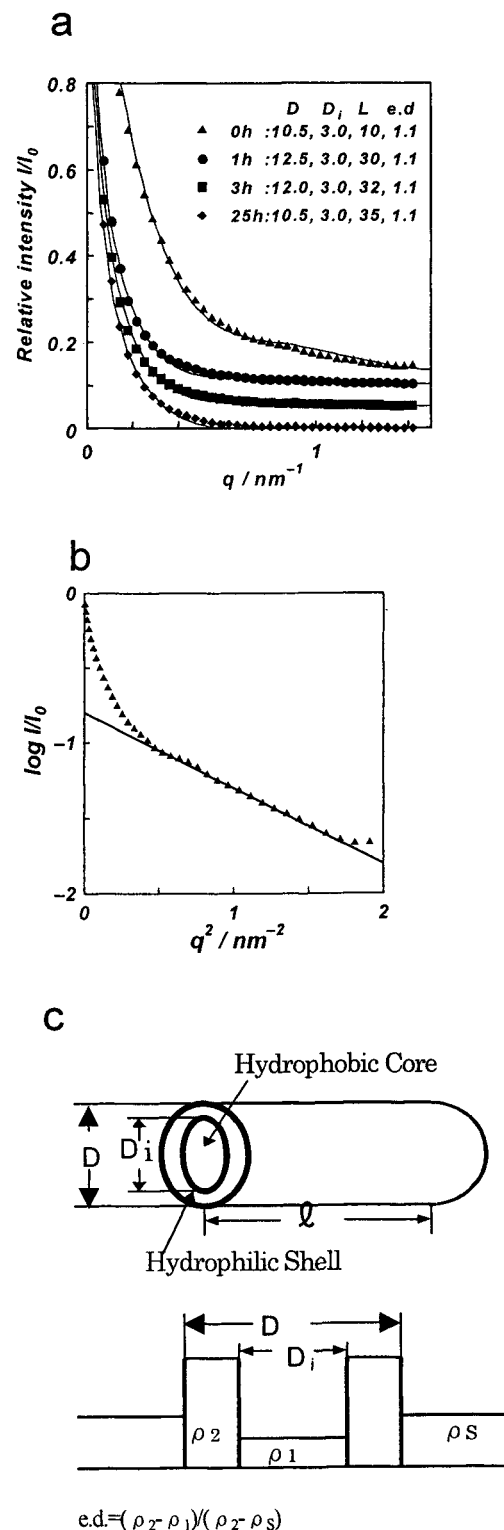
$$e.d.=(\rho_2-\rho_1)/(\rho_2-\rho_s)$$

Figure 1 a) SAXS results of liquid samples during the formation processes. I : scattering intensity, q : scattering vector b) Guinier type plot of data at 0 h. c) Assumed coaxial double cylinder and electron density profile.

nanotubes

Surfactant molecules in titania nanotubes can be removed from mesopores by washing with alcohol. We controlled the alcohol content by the centrifugation speed, when the sample was separated from the alcohol solution by centrifugation. We chose the best alcohol content, which gave the highest short-circuit photocurrent density because the open-circuit voltage was almost constant around 0.6 V.
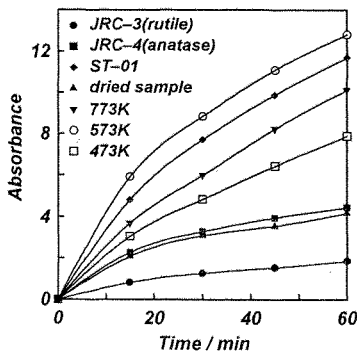

Figure 3 Photo-catalytic activities of titania nanotubes in comparison with those of the standard titania particles.
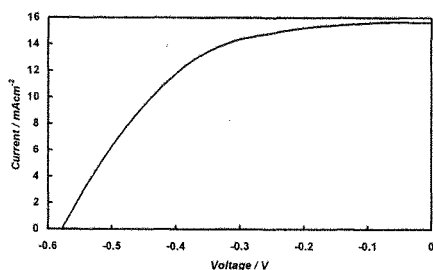

Figure 4 An example of photo-current-voltage characteristics of a cell made of titania nanotubes.

Figure 4 shows an example of photo-current-voltage characteristics of a cell made of the titania nanotubes. The film thickness was 4 μm, and the cell size was 0.5 cm×0.5 cm. The obtained short-circuit photocurrent density was 15.3 mA/cm², and the open-circuit voltage was 0.58 V. The light-to-electric energy conversion yield was 4.88 %, and the fill factor was 0.54.

In order to compare the cell composed of titania nanotubes with a cell composed of the standard titania particles P-25, we measured the photo-current-voltage characteristics of the cell made of P-25. The open voltage was about 0.6 V, which was the same as the cell made of titania nanotubes. Thus, we can evaluate the efficiency of the cell by mainly comparing the values of the current density.

Figure 5 shows the short-circuit photocurrent density obtained from the cells made of titania nanotubes, together with those of P-25, against the film thickness. In the thin film region, the photocurrent density of the cell made of titania nanotubes was more than two times higher than that of P-25. The high photocurrent density in the thin film region might be attributed to the significant decrease in the inter-crystalline contact of titania by using mono-crystalline titania nanotubes with a high aspect ratio.

Ceria Nanotubes

Ceria nanotubes were synthesized using an alcoholic solution of tetra-buthoxycerium and a LAHC aqueous solution in the same way as the formation of titania nanotubes as shown in Figure 6. XRD measurement showed that the nanotubes had

cubic crystal. The nitrogen adsorption isotherm showed typical IUPAC type IV pattern, and the BET surface area was 60 m²/g.
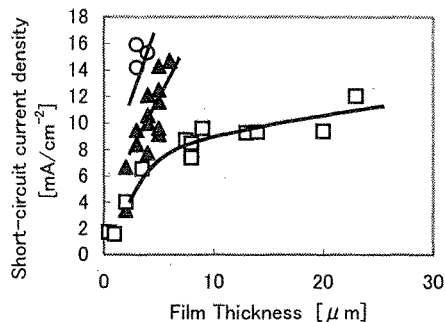

Figure 5 Relationship between the short-circuit photocurrent density and the film thickness. ◯: titania nanotubes 0.5 cmx0.5cm, ▲: titania nanotubes 1 cmx1 cm, □: P-25 1 cmx1 cm
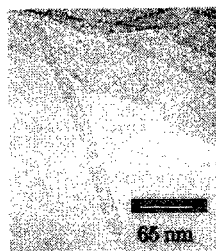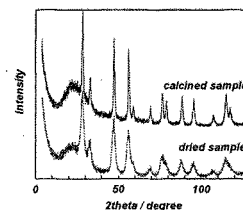

Figure 6 TEM image of ceria nanotubes.

Figure 7 XRD of ceria sample

REFERENCES
[1] C. T. Kresge, M. E. Leonowicz, W. J. Roth, J. C. Vartuli, J. S. Beck, *Nature*, 359, 710-712(1992)
[2] J. S. Beck, et al. , *J. Am. Chem. Soc.*, 114, 10834-10843 (1992)
[3] M. Adachi, T. Harada, M. Harada, *Langmuir*, 15, 7097-7100(1999)
[4] M. Adachi, T. Harada, M. Harada, *Langmuir*, 16, 2376-2384(2000)
[5] "Characterization of Nanophase Materials", Ed. By Z.L.Wang,. Wiley-VCH, Weinheim (2000)
[6] "Physics and Chemistry of Nanostructured Materials", Ed. By S.Yang, P, Sheng, Taler & Francis, London New York(2000)
[7] "Molecular Nanostructures", Ed. By H.Kuzmany, J.Fink, M. Mehring, S,Roth World Scientific, Singapore (1998)
[8] H.Nakamura, Y.Matsui, *J Am Chem Soc*, 117, 2651-2652(1995)
[9] H-P.Lin, C-Y.Mou, *Science*, 273, 765-768(1996)
[10] M.Trau,N. Yao, E.Kim, Y.Xia, G.M.Whitesides, L.A.Aksay, *Nature*, 390, 674-676(1997)
[11] H.Masuda, K.Fukuda, *Science*, 268, 1466-1468(1995)
[12] H.Masuda, H.Yamada, M.Satoh, H.Asoh, M.Nakao, T.Tamamura, *Appl Phys Lett*, 71, 2770-2772(1997)
[13] W.Shenton, T.Douglas, M.Young, G.Stubbs, S.Mann, *Adv. Mater.*, 11, 253-256(1999)
[14] Y.Ono, K.Nakanishi, M.Sano, Y.Kanekiyo, K.Inoue, J.Hojo, S.Shinkai, *Chem Commun*, 1477-1478(1998)
[15] M. Adachi, Y. Murata, M. Harada, S. Yoshikawa, *Chemistry Letters*, 942-943(2000)
[16] M. K. Nazeeruddin, A. Kay, I. Rodicio, R. Humphry-Baker, E. Müller, P. Liska, N. Vlachopoulos, M. Grätzel, *J. Am. Chem. Soc.*, 115, 6382-6390(1993)

at 313 K, and the solution became transparent. Turning to the transparent solution means that the precipitates were finely divided into small materials, which were smaller than the wavelength of light. When the temperature of the transparent solution was increased to 353 K, the reaction started. After 3 h from the start of reaction, the solution became a gel. After 5 h, the hard gel became weak, and a liquid phase appeared. After 25 h, the solution became a white gel again with a transparent yellow liquid thin layer on the gel, and this state was maintained for three days.

The variation in SAXS pattern with time is shown in Figure 1a. Time 0 h represents the state of the transparent solution after complete dissolution of precipitates at 313 K, and 1 h, 3 h, and 25 h are the times after the start of reaction at 353 K. The logarithmic values of the observed scattering intensity log I were re-plotted against the square of scattering vector q^2 in Guinier type as shown in Figure 1b, and linear relationships between log I and q^2 were obtained for all data in the high q^2 range, indicating particle formation. The particle radius for each time was determined as 2.28 nm for 0 h, 2.17 nm for 1 h, 2.20 nm for 3h, and 1.90 nm for 25 h from the slope of the straight line in the Guinier type plot. The amount of particles became small after the start of the reaction at 353 K. The scattering intensity due to particles (straight line in Figure 1b) was subtracted from the observed intensity, and the obtained difference intensity was analyzed. For the SAXS analysis of the rod shaped assembly, we assumed co-axial double cylinders with an outer hydrophilic shell (outer diameter D: electron density ρ_2), and an inner hydrophobic core (diameter D_i: electron density ρ_1). The rod length is ℓ, the length distribution being $(1/L)\exp(-\ell/L)$ (see Figure 1c). ρ_s is the electron density of the aqueous solution. The analyzed results are shown in Figure 1a. At 0h, the outer diameter D was 10.5 nm, inner diameter D_i was 3 nm, and length was 10 nm, showing formation of short rod. After the temperature became 353 K, length became large, i.e., 30 to 35 nm, indicating to become real rod keeping the diameter constant.

Figure 2a shows a TEM image of nanotubes in a gel sample. We can see long nanotubes (diameter 10 nm, length 200 nm) as well as short ones (diameter 10 nm, length 30 nm). SAXS results indicate that these short nanotubes are predominant. Electron diffraction patterns of these nanotubes show the Debye-Scherrer rings of anatase. A TEM image of the calcined sample in the ODA / TIPT with ACA system is shown in Figure 2b. We can see lattice image of the nanotubes, which clearly shows that nanotubes are mono-crystals of anatase. The electron diffraction pattern exhibited in Figure 2c also shows that nanotubes are crystals of anatase. These TEM images and electron diffractions clearly show that titania nanotubes are mono-crystals of anatase. This is a remarkable feature of this titania nanotube.

The nitrogen adsorption isotherm of a calcined sample at 673 K shows a typical IUPAC type IV pattern, indicating that an open mesosize tubular shape was formed. BET surface area was in the range from 150 to 200 m²/g. The peak pore diameter obtained was as 4.6 nm, which was a similar value to that obtained from TEM images and SAXS data.

Figure 3 shows the photo-catalytic activity of titania nanotubes, together with some standard photo-catalysts of TiO_2. JRC-3 has a rutile crystalline structure and JRC-4 has a mainly anatase structure. Both nano-crystalline particles were supplied by the Catalysis Society of Japan. JRC-4 corresponds to Degussa P-25, whose BET surface area is about 55 m²/g. ST-01 is known as the highest photo-catalytic active commercially available particle from Ishihara, Co. Ltd and has

very large surface area, i.e., 300 m²/g. The activity depends significantly on both the calcination period and calcination temperature. The best activity at present was obtained for the sample calcined at 573 K for 24 h. The best activity was 7 times higher than that of JRC-3, 2.8 times higher than that of JRC-4,
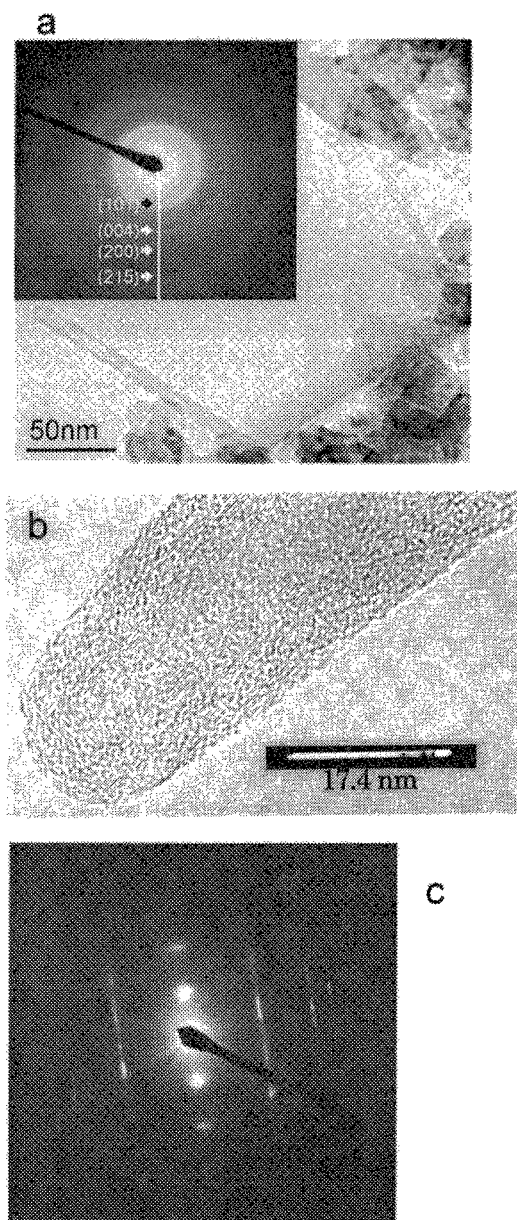
Figure 2 a) TEM image of titania nanotubes in gel sample. Inset: Electron diffraction of titania nanotubes. b) TEM image of calcined titania nanotubes at 773 K for 4 h in ODA / TIPT with ACA system. c) Electron diffraction pattern of the calcined titania nanotubes.

and even higher than ST-01. High photocatalytic activity of our titania sample is attributed to the large surface area, i.e., 150 to 200 m²/g, but our sample showed higher activity than ST-01. (300 m²/g) Thus, some other factor must contribute to the high photocatalytic activity. We can conclude that very photo-catalytic active titania nanotubes can be made by the present method.

Characteristics of the thin film electrode made of titania